PHYSICAL REVIEW B VOLUME 22, NUMBER 10 15 NOVEMBER 1980

Study of the localized vibrations of boron in heavily doped Si

Meera Chandrasekhar*
Research Reactor and Department of Physics, University of Missouri, Columbia, Missouri 65211

H. R. Chandrasekhar*
Department of Physics, University of Missouri, Columbia, Missouri 65211

M. Grimsditch and M. Cardona
Max-Planck-Institut für Festkörperforschung, 7000 Stuttgart 80, Federal Republic of Germany
(Received 27 March 1980)

We have studied the localized vibrational modes of boron in heavily doped Si using Raman scattering for carrier concentrations of 5×10^{18} to 1.5×10^{20} cm^{-3}. The line shapes and positions of the local mode and optic-phonon spectra due to interaction with the intervalence band continuum of electronic transitions are studied for different exciting frequencies. The local mode was also examined under uniaxial stress and was found to behave in a fashion similar to that of the optic phonon except for a larger hydrostatic shift, which seems due to the larger local compressibility in the region of the smaller boron atom.

I. INTRODUCTION

Localized vibrational modes of boron in silicon have been studied theoretically[1] and experimentally, the latter both by infrared absorption[2,3] and Raman scattering.[4,5] Boron, being a lighter atom than Si, produces a local vibrational mode that occurs at a frequency higher than that of the optic phonon (520 cm^{-1}), at 620 cm^{-1} for ^{11}B and 644 cm^{-1} for ^{10}B. These local modes are observable in Raman scattering at boron concentrations of ~10^{19} cm^{-3} or higher. Since boron acts as an acceptor in Si, an equal number of free holes is produced (assuming that all boron atoms are electrically active), pushing the Fermi level out of the band gap into the valence bands at a concentration near 10^{19} cm^{-3}. Raman-active intervalence band transitions can then occur: They produce a broad scattering continuum. The energies of both the optic phonon and the local modes of boron fall within this continuum and a Fano-type interference[6] takes place, which results in asymmetric line shapes for both the phonon[7] and the local modes.[5] The Raman spectrum of the local modes of boron as a function of incident laser frequency for heavily doped p-Si ($p\simeq4\times10^{20}$ cm^{-3}) has been studied by Cerdeira *et al.*[5] We extend this study to a range of carrier concentrations ($p\simeq5\times10^{18}$ to 1.5×10^{20} cm^{-3}) and perform an analysis of the parameters involved in the line shape and position of the boron local mode. The changes in scattering intensity of the phonon and local mode as a function of doping are investigated. We have also studied the local mode of ^{11}B as a function of uniaxial stress along the [001] and [111] crystal directions for a concentration of $p=1.5\times10^{19}$ cm^{-3}, and find that the hydrostatic shift in the frequency of the local mode is almost twice that of the optic phonon. We attribute this to the high local compressibility in the vicinity of the boron atom, which in turn arises from the fact that a boron atom is smaller than a silicon atom.

II. EXPERIMENTAL DETAILS

Raman spectra were taken at room temperature in the backscattering configuration standard for opaque materials. Spectra Physics Ar^+ and Kr^+ lasers were used to obtain the exciting radiation. A Spex triple monochromator with a wave-number drive and a cooled photomultiplier equipped with photon counting electronics were used for detection, in conjunction with a multichannel analyzer for data storage. Counting times of 2–5 sec per channel were utilized to record spectra of the zone center phonon and 30–80 sec per channel for the local modes. The stress apparatus employed was equipped with a digital readout as has been described previously in the literature.[8] Typically, compressive stresses up to 20 kbar were reached. A neon lamp was used for wavelength reference and calibration purposes.

Samples of Si were cut from single crystals, and x ray oriented to within 1°. For stress measurements the samples were cut into bars of $20\times1.3\times1.3$ mm^3, and the stress was applied along their length. The face used for scattering was polished with 0.3 μm alumina, polish etched with Syton[9] for 10 min, and etched in HF for 1 min.

III. THEORETICAL DESCRIPTION

The presence of holes in the valence bands permits Raman-active interband transitions between the top valence bands.[7] At acceptor dopings of

10^{19} cm^{-3} and higher the energies of both the optic phonon and the local modes of boron fall within the energy range of the continuum, and a discrete-continuum interaction takes place, resulting in typically asymmetric Fano-type line shapes for both the optic phonon[7] and the local modes of boron.[5] Based on the Fano theory, the line shape of the optic phonon can be written in the form

$$I(\omega)=A\frac{(q_p+\epsilon_p)^2}{1+\epsilon_p^2}, \tag{1a}$$

where

$$\epsilon_p=\frac{\omega-\omega_p-\Delta\omega_p}{\Gamma_p}, \tag{1b}$$

q_p is the asymmetry parameter, ω_p is the frequency of the optic phonon in pure Si, $\omega_p+\Delta\omega_p$ is the frequency in doped Si, Γ_p is the linewidth, and A is a constant. An identical expression describes the Fano-type line shape for the local mode of ^{11}B, where we replace A, q_p, ω_p, $\Delta\omega_p$, and Γ_p by the equivalent parameters for the local mode B, q_L, ω_L, $\Delta\omega_L$, and Γ_L. The ^{10}B isotope has a local mode 24 cm^{-1} higher in frequency[2,3] than the ^{11}B local mode, but is four times weaker in intensity since it has a relative abundance of about 0.2. Within experimental error the Fano parameters for ^{11}B and ^{10}B local modes are the same.

The three Fano parameters of the optic phonon are related to the microscopic properties of the crystal in the following manner.[7,10] Writing the linewidth Γ as the sum of the intrinsic linewidth Γ' plus the line broadening due to the interaction with the continuum Γ'' we find

$$q_p=(V_pT_p/T_e+\Delta\omega_p)/\Gamma_p'', \tag{2a}$$

$$\Gamma_p''=\pi V_p^2D_d(\omega_p), \tag{2b}$$

$$\Delta\omega_p=V_p^2\mathrm{P}\int D_d(\omega')\left(\frac{1}{\omega_p-\omega'}-\frac{1}{-\omega_p-\omega'}\right)d\omega', \tag{2c}$$

where V_p is an average matrix element for the hole-phonon interaction, and T_p and T_e are the Raman matrix elements between the ground and excited states of the phonon and the hole (the latter also an average). $D_d(\omega)$ is the joint density of states of the electronic continuum for direct transitions and P represents the principal part of the integral. The Fano parameters of the local mode are defined in a similar manner:

$$q_L=(V_LT_L/T_e+\Delta\omega_L)/\Gamma_L'', \tag{3a}$$

$$\Gamma_L''=\pi V_L^2D_d(\omega_L), \tag{3b}$$

$$\Delta\omega_L=V_L^2\mathrm{P}\int D_d(\omega')\left(\frac{1}{\omega_L-\omega'}-\frac{1}{-\omega_L-\omega'}\right)d\omega' \tag{3c}$$

V_L is the hole–local-mode matrix element and T_L is the Raman matrix element of the local mode. The electronic matrix element T_e is assumed to be the same for all electronic transitions since these occur over a relatively small region of the Brillouin zone. The density of states $D_d(\omega)$, which is the density of states for *direct transitions* as required by the Raman scattering selection rules, can also be assumed to be the same in Eqs. (2) and (3). V_p and V_L are the phonon and local-mode deformation potentials at the valence bands in Si, and are defined analogously to the hole-phonon matrix element given by Eq. (4-62) in Ref. 11 [however, V_L requires a renormalization as for the local-mode indirect transitions are possible, see Eq. (8)]. The frequency shifts and broadenings $\Delta\omega_p$, $\Delta\omega_L$ and Γ_p, Γ_L are real and imaginary parts of the self-energy due to the interaction with the free holes in the conduction band and are independent of the exciting laser frequency Ω, but change with carrier concentration via the density of states $D_d(\omega)$, which in turn depends on the Fermi level. The asymmetry parameters q_p, q_L, however, change with the exciting frequency via the Raman matrix elements T_p, T_L, and T_e:

$$T_p\sim P(\Omega)\Omega^2, \tag{4a}$$

$$T_e\sim\left(\frac{1}{h\Omega+E_g}-\frac{1}{h\Omega-E_g}\right), \tag{4b}$$

where $E_g=3.4$ eV is the energy of the direct gap at the center of the Brillouin zone and $P(\Omega)$ the Raman tensor.[12,13] The expression for T_L is not known, but in a rough approximation it can be expected to behave similarly to T_p. Apart from a dependence on exciting frequency, q_p and q_L also vary with the carrier concentration via the frequency shifts and line broadenings.

The interpretation of the parameters determined from the spectra of the local mode is somewhat complicated by the fact that the local mode can also couple to electronic transitions that do *not* conserve k. Because these indirect transitions are Raman inactive the net result is to effectively increase the intrinsic linewidth and shift the line position. Experimentally we are unable to separate the line broadenings and shifts which arise from indirect transitions and which lead to no line asymmetry from those arising from direct transitions and which produce the Fano line shape.

IV. RESULTS AND DISCUSSION

A. Concentration and exciting frequency dependence

The Raman spectra of the zone-center optic phonon and the local modes of boron were mea-

sured at room temperature for samples with carrier concentrations ranging from 5×10^{18} to 1.5×10^{20} cm^{-3} and various laser frequencies.

The Raman spectra in the region of the optic phonon for different boron concentrations are shown in Fig. 1. The solid lines through the data points are least-square computer fits to the Fano expression of Eq. (1). The adjustable parameters in the fit are A, q_p, $\omega_p+\Delta\omega_p$, and Γ_p. After the Fano parameters of the optic phonon were obtained from the fit, the spectrum of the local mode was then fitted to the expression

$$I_L(\omega)=\frac{A(q_p+\epsilon_p)^2}{1+\epsilon_p^2}+B\left(\frac{4}{5}\frac{(q_L+\epsilon_L)^2}{1+\epsilon_L^2}+\frac{1}{5}\frac{(q_L+\epsilon_L')^2}{1+\epsilon_L'^2}\right)+C, \tag{5}$$

where

$$\epsilon_L=\frac{\omega-\omega_L-\Delta\omega_L}{\Gamma_L} \tag{6a}$$

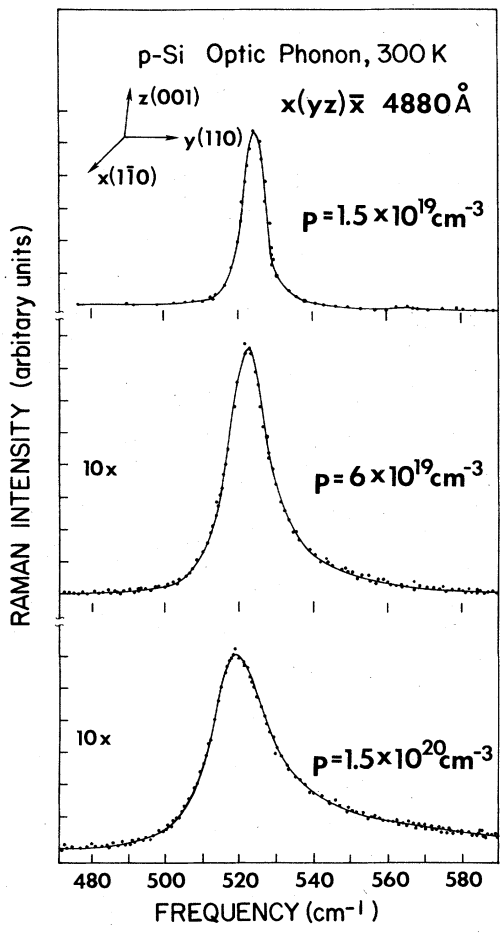

FIG. 1. Optic phonon for several concentrations, data, and fit to Eq. (1). Exciting wavelength is 4880 Å.

for the ^{11}B isotope and

$$\epsilon_L'=\frac{\omega-\omega_L-\Delta\omega_L-\Delta}{\Gamma_L} \tag{6b}$$

for the ^{10}B isotope. In Eq. (5) A and B are amplitude terms for phonon and local modes and C is a constant that accounts for possible stray light and noninteracting electronic continuum. The numerical factors $\frac{4}{5}$ and $\frac{1}{5}$ reflect the natural abundances of the two isotopes. In the least-square fit to the data using Eq. (5), the values of q_p, $\omega_p+\Delta\omega_p$, and Γ_p obtained from the fit to the optic phonon for the same carrier concentration and exciting wavelength were used, while A, B, C, q_L, Γ_L, $\omega_L+\Delta\omega_L$ and Δ were used as adjustable parameters. It was found that $\Delta\simeq 24\pm1$ cm^{-1} for all carrier concentrations, a value in agreement with previous measurements.[2,3,5] For all the concentrations it was important to use the fact that the local modes are weak structures superimposed on the decreasing tail on the high-frequency side of the optic phonon. However, the Fano parameters obtained from the fit to the local-mode spectrum are relatively insensitive to Γ_p and q_p. Figure 2 shows the Raman spectra of the local

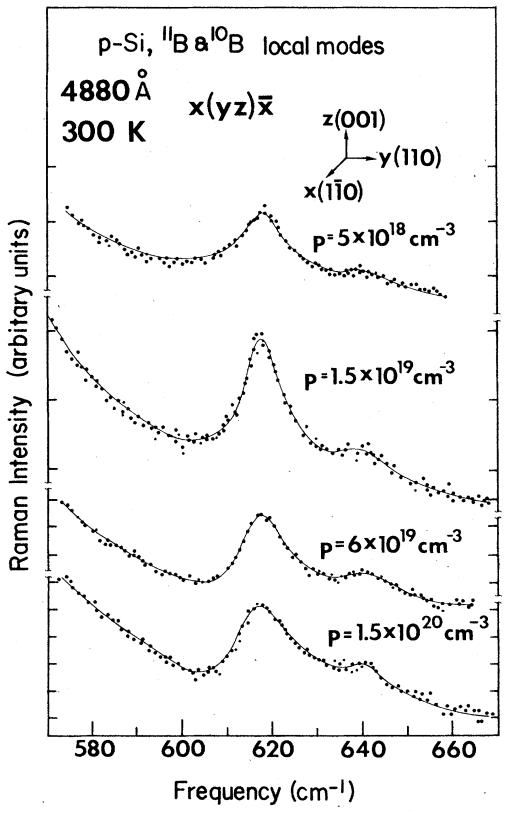

FIG. 2. Local modes of boron for different concentrations, data, and fit to Fano function [Eq. (5)]. Exciting wavelength is 4880 Å.

TABLE I. Fano parameters of the optic phonon and ^{11}B local mode in Si for different exciting frequencies and carrier concentrations.

Carrier concentration (cm^{-3})	Exciting wavelength (Å)	Optic Phonon q_p	Γ_p (cm^{-1})	$\omega_p + \Delta\omega_p$ (cm^{-1})	^{11}B local mode q_L	Γ_L (cm^{-1})	$\omega_L + \Delta\omega_L$ (cm^{-1})
4×10^{20} [a]	4579	4.54	12.4±0.5	512±2	1.82	8.0±1.5	615±2
	5145	2.57	11.8±0.5	511±2	1.16	7.4±1.5	614±2
	6471	0.55	12.6±0.5	509±2	0.15	10.0±1.5	613±2
			average	average		average	average
			12.3±0.5	510.7±1.5		8.5±1.8	614±2
1.5×10^{20}	4880	6.0	9.2	516.7	2.7	7.3	614.8
	6471	1.8	8.5	514.8	0.93	6.4	614.2
			average	average		average	average
			8.85±0.5	515.7		6.9±0.6	614.6
6×10^{19}	4880	10	6.2	519.7	3.2	6.4	615.8
1.5×10^{19}	4880	44	3.1	520.2	8	6.0	617.1
	6471	20.0	2.65	520.2	5.8	5.9	617.3
			average	average		average	average
			2.88	520.2		5.95	617.2
5×10^{18}	4880	200	1.8	520	33	6.8±1.0	618
Pure Si (10^{13})			1.5	520.0		5.5 [b]	620 [b]

[a] Cerdeira *et al.*, Ref. 5.
[b] J. Angress *et al.*, Ref. 3.

mode and the fits obtained using Eq. (5).

The values of the Fano parameters obtained for both the optic phonon and the local mode of ^{11}B for several concentrations and exciting frequencies are given in Table I. Included in the table are values obtained by Cerdeira *et al.*[5] for a concentration of $p = 4\times10^{20}$ cm^{-3}, the broadening and frequency of the phonon in pure Si,[12] and the broadening and frequency of the local mode of ^{11}B obtained by infrared absorption in a phosphorus compensated sample by Angress *et al.*[3] In Table I we also list average values of Γ_p, Γ_L and ω_p, ω_L obtained for different exciting wavelengths but the same carrier concentration, since these quantities are independent of the frequency of exciting radiation used. The parameters Γ_p and $\Delta\omega_p$ have been measured[5] and interpreted[5,11] and hence no more will be said about them here.

We list in Table II the values of V_pT_p/T_e obtained from the Fano parameters listed in Table I, using Eq. (2a). The frequency of the optic phonon and its intrinsic linewidth were taken from the values listed under "pure" Si in Table I.

We note from Table II that V_pT_p/T_e is independent of carrier concentration and depends on exciting frequency alone, in agreement with the description in Sec. III. The average value for each exciting frequency Ω is plotted versus exciting energy in Fig. 3. From Eqs. (4a) and (4b) the Ω dependence of V_pT_p/T_e is

$$\frac{V_pT_p}{T_e}(\Omega) \simeq DP(\Omega)(\hbar\Omega)^2\left(\frac{1}{\hbar\Omega+E_g}-\frac{1}{\hbar\Omega-E_g}\right)^{-1} \tag{7}$$

assuming V_p to be independent of Ω. Here D is a fitting factor. Using the dispersion of the theoretically calculated values of $P(\Omega)$ from Ref. 12, we obtain the solid line which represents the experimental behavior rather well. The experimental

TABLE II. V_pT_p/T_e for different concentrations and exciting wavelengths. From Table I, $\Gamma_p'' = \Gamma_p - 1.5$ cm^{-1}.

Exciting wavelength (Å)	Concentration (cm^{-3})	V_pT_p/T_e (cm^{-1})
4579	4×10^{20}	58.3
4880	1.5×10^{20}	48.3
	6×10^{19}	47.3
	1.5×10^{19}	60.5
		average (weighted) 49.3
5145	4×10^{20}	37.1
6471	4×10^{20}	15.2
	1.5×10^{20}	17.5
	1.5×10^{19}	27.4
		average (weighted) 17.9

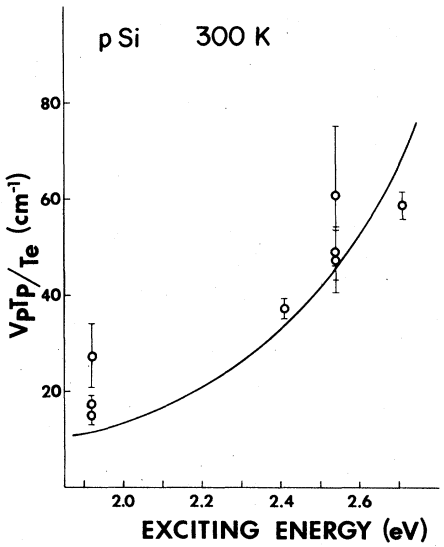

FIG. 3. $V_p T_p/T_e$ obtained from the Fano parameters as a function of exciting energy $\hbar\Omega$. Fit is obtained from Eq. (7) using a scaling factor and denoted by the dashed line.

values of $P(\Omega)$ would give a somewhat steeper dependence of $V_p T_p/T_e$ on Ω in Fig. 3. This fact can be compensated by increasing E_g, i.e., by including the $\Gamma_{25'}-\Gamma_{2'}$ gap (=4.1 eV) in the resonant process of Eq. (7).

The procedure just described for obtaining $T_p V_p/T_e$ for the phonon cannot be utilized for the local mode because, as mentioned earlier, the line broadening Γ'' due to direct, Raman-active transitions, entering in Eq. (3a), is not know from the experimental results. However, following Ref. 5, we note the analogous frequency dependence of q_p and q_L and conclude that the frequency dependence of T_L is similar to that of T_p.

B. Linewidth analysis

The linewidth of the local mode as a function of doping is shown in Fig. 4. In order to calculate the linewidth we use Eq. (3b) but consider all possible transitions without the restriction of $\vec{k}$ conservation. This assumption is legitimate because the local mode has no well defined $\vec{k}$ vector and can hence decay into electronic excitations of any wave vector. Furthermore, because of the extreme localization of the local-mode vibration, it is legitimate to assume that its Fourier decomposition contains all q vectors of the Brillouin zone

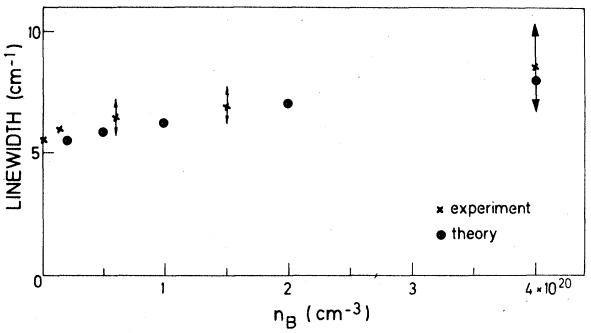

FIG. 4. Linewidth of the local mode versus boron concentration.

with equal amplitude. Because of the similarity of a boron and silicon vibrations we write

$$V_L = (V_p/\sqrt{N})\alpha\,, \tag{8}$$

where N is the number of primitive cells per unit volume, equal to the number of q vectors in the Fourier decomposition of the boron vibration, and α is a fitting parameter which can be expected to be somewhat larger than one because the amplitude of vibration of a boron atom is larger than that of an Si atom as a result of the mass difference [$\alpha \simeq (M_{Si}/M_B)^{1/2} = 1.7$]. The value of V_p^2 from Eq. (4-62) of Ref. 11 is 4.8×10^{-25} eV^2 cm^3.

The density of states for indirect transitions is calculated on the basis of parabolic bands. For one band of effective mass m_i the density of states is given by

$$D_i(E) = (m_i^{3/2}/\sqrt{2}\,\pi^2\hbar^3)\sqrt{E}\,. \tag{9}$$

If the Fermi energy (measured from the top of the valence band) is ϵ_F the density of indirect transitions from band i to band j is (we assume $T \simeq 0$)

$$D_{ij}(\epsilon) = 2\int_{\epsilon_F}^{\epsilon_M} D_i(\chi) D_j^*(\chi-\epsilon)\,d\chi, \tag{10}$$

where

$$D_j^* = \begin{cases} D_j & \text{if } \chi-\epsilon < \epsilon_F \\ 0 & \text{if } \chi-\epsilon > \epsilon_F \end{cases}, \tag{11}$$

and the prefactor of 2 is due to the spin degeneracy. ϵ_M is a cut-off energy which represents the termination of the bands at the edge of the Brillouin zone. Provided $\epsilon_M > 2\epsilon_F$ the integral of Eq. (10) yields (independent of ϵ_M)

$$D_{ij}(\epsilon) = \frac{(m_i m_j)^{3/2}}{4\pi^4\hbar^6}\left[2\epsilon_F^{3/2}[(\epsilon_F+\epsilon)^{1/2}-(\epsilon_F-\epsilon)^{1/2}] + \epsilon\sqrt{\epsilon_F} + \epsilon\sqrt{\epsilon_F}[(\epsilon_F+\epsilon)^{1/2}+(\epsilon_F-\epsilon)^{1/2}] + \epsilon^2 \ln\left(\frac{(\epsilon_F-\epsilon)^{1/2}+\epsilon_F^{1/2}}{\epsilon_F^{1/2}+(\epsilon_F+\epsilon)^{1/2}}\right)\right] \quad \text{if } \epsilon < \epsilon_F \tag{12}$$

or

$$D_{ij}(\epsilon)=\frac{(m_i m_j)^{3/2}}{4\pi^4\hbar^6}\left[\sqrt{\epsilon_F}(\epsilon_F+\epsilon)^{1/2}(2\epsilon_F+\epsilon)+\epsilon^2\ln\left(\frac{\sqrt{\epsilon}}{\epsilon_F^{1/2}+(\epsilon_F+\epsilon)^{1/2}}\right)\right] \quad \text{if } \epsilon>\epsilon_F\,. \tag{13}$$

With Eqs. (3b), (12), and (13) the masses of the heavy, light and spin-orbit-split holes of the valence band (i.e., $0.73m_e$, $0.10m_e$, and $0.25m_e$)[14] and the Fermi energies as a function of concentration from Ref. 11, we obtain the values of Γ shown in Fig. 4. The parameter α of Eq. (8) has been chosen to be 2.4 in order to fit the experimental results at $\sim 2\times10^{20}$ cm^{-3} and the "natural" linewidth of 5.5 cm^{-1} (Ref. 12) has been added to our results.

C. Line shift

The shift of the mode as a function of doping can be calculated in an analogous manner starting with Eq. (2c). The integral has been carried out numerically, and the experimental and calculated results are shown in Fig. 5 (a complicated analytical expression can, however, be written down if desired). The parameter α has been chosen to be 1 and the cutoff energy $\epsilon_M=10$ eV. A value of α somewhat different from the one obtained from the line width can be attributed to the nonparabolicity of the valence bands.

D. Intensity measurements

Using Eqs. (1a) and (1b) it is easy to show that the integrated intensity (I_p) which is attributable to the phonon is $Aq_p^2\Gamma_p$. Furthermore, since A is the intensity observed for ω far from ω_p it can be concluded that

$$A\propto T_e^2 D_d(\omega)\,. \tag{14}$$

Using Eqs. (2) and (14) I_p can be written as

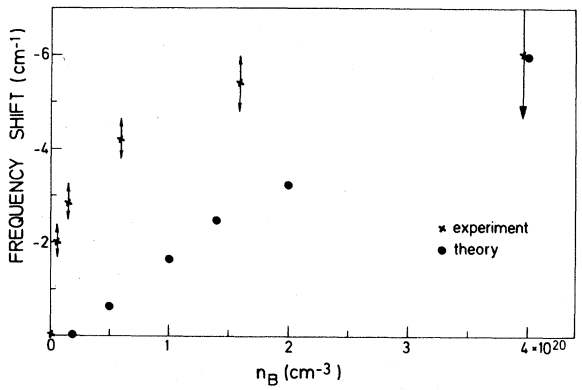

FIG. 5. Frequency shift of local mode versus boron concentration.

$$I_p=\frac{T_e^2}{V_p^2}\left(\frac{V_pT_p}{T_e}+\Delta\omega_p\right)^2. \tag{15}$$

This equation predicts the rather surprising effect that the intensity of the optical phonon is modified through its frequency shift with doping. This means that a Raman-inactive mode ($T_p=0$) may become active through interaction with the Raman-active electronic continuum.

In order to verify the above conclusion we made a comparison of the intensities of the zone-center optic phonon in pure and 1.7×10^{20} boron-doped silicon samples. The experiment was carried out at 6471, 5681, and 4880 Å and the results are presented in Table III, together with those calculated using Eq. (15), the values of V_pT_p/T_e from Fig. 3, and $\Delta\omega=-6$ cm^{-1} interpolated from Table I. Considering the errors of the experimental determinations (~20%) and uncertainties in the parameters entering the calculation the agreement can be seen to be extremely good.

The intensity of the local mode was compared to that of the phonon for various dopings. Because of the larger errors associated with the determination of parameters of the local mode, no changes in the intensity ratios were detectable as a function of wavelength even though, according to the arguments given in the preceding paragraph, changes could be expected. The average values of the scattered intensity per boron atom divided by the scattered intensity per silicon atom for different wavelengths are shown in Fig. 6. From the simple argument that the Raman-scattering matrix element T is proportional to the deformation potential V we would expect the intensity ratio to be α^2 with only a weak concentration dependence determined by the phonon as shown in Table III. Our estimates of α^2 lie between 1 and 5.7, in relatively good agreement with the intensity ratio at large dopings. The increase of the local-mode intensity at low dopings can be attributed to an additional scattering mechanism due to the Coulomb field associated with the boron atom. This field is screened at large dopings by the free carriers. The additional scattering should be of the form (for each single B atom)

$$V\propto\frac{1}{q^2+q_{\mathrm{TF}}^2}\,, \tag{16}$$

where q_{T}^{-1} is the Thomas-Fermi screening radius,[15] proportional to the $-\frac{1}{6}$ power of the hole

TABLE III. Ratio (R) of the intensity of the zone-center optical phonon of doped (1.7×10^{20} cm^{-3}) to that of pure Si as a function of wavelength.

λ (Å)	6471	5681	4880
R_{expt}	0.32	0.53	0.63
R_{calc}	0.21	0.47	0.75

density, i.e.,

$$q_{TF} \propto n_B^{1/6}, \tag{17}$$

where n_B is the boron concentration. In Fig. 6 we have fitted the ratio of the local mode to the phonon intensities (normalized to one atom each) to the equation

$$\frac{A_L q_L^2 \Gamma_L n_{Si}}{A_p q_p^2 \Gamma_p n_B} = \beta n_B^{-2/3} + \gamma, \tag{18}$$

which results from the considerations above. The fit, which is quite satisfactory, was obtained with the parameters $\beta = 1.7\times10^{14}$ cm^{-2} and $\gamma = 8$. The value of γ so obtained falls close to the range 1–5.7 estimated above. We do not attempt in the present work an estimate of β, which should be made on the basis of a microscopic theory of the local modes and the impurity scattering. We note that the additional electrostatic scattering of Eq. (16) has not been included in the results of Secs. IV C and IV D, as in these sections indirect transitions with $q \gg q_{TF}$ play the decisive role. The effect of such electrostatic scattering on the real and imaginary parts of the local-mode energy has been recently investigated[16] within a free-electron model (only intraband transitions). Because of the uncertainty of the volume polarizability to be used in the calculation it is not possible to make a quantitative estimate of the *magnitude* of this term. The functional dependence of the observed frequency shift suffices, however, to explain the difference between the present theory and the experiment in Fig. 5.[16]

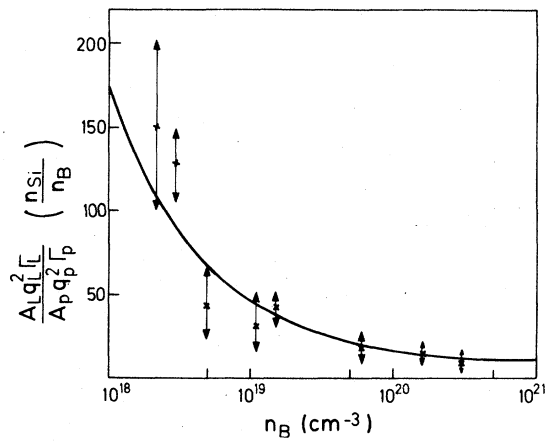

FIG. 6. Ratio of scattered intensities of the local mode and optic phonon normalized to a single atom versus boron concentration.

E. Dependence on uniaxial stress

The spectra of the local modes for the sample of boron concentration 1.5×10^{19} cm^{-3} were studied under compressive uniaxial stresses up to 20 kbar applied along the [001] and [111] crystal directions for an exciting wavelength of 4880 Å. The behavior of the local modes is similar to that of the optic phonon under uniaxial stress[17]: a linear frequency shift to higher frequencies due to the hydrostatic component of the stress and a splitting of the threefold degeneracy into a doublet and a singlet due to the shear component for both stress directions.

We plot in Fig. 7(a) the frequency of the optic phonon for a concentration $p = 1.5\times10^{19}$ cm^{-3} versus stress X for both directions of applied stress. The phonon doublet (singlet) is marked ω_{pd} (ω_{ps}) and the frequency shift due to the hydrostatic component of the stress (obtained from the center of gravity of the two components) is denoted by the dashed line ω_{ph}. In Fig. 7(b) we plot the frequency of the local modes versus stress for the same carrier concentration. The doublet, singlet, and hydrostatic shifts are marked ω_{Ld}, ω_{Ls}, and ω_{Lh}, respectively. For both the phonon and the local modes the doublet and singlet were isolated by a proper choice of polarizations[17]: For a [001] stress axis the doublet is observed when the polarization of the incident light is parallel and the scattered light perpendicular to the stress axis ($\parallel,\perp$), while the singlet is observed in the ($\perp,\perp$) polarization. For a [111] stress axis the doublet is seen in the ($\parallel,\perp$) and the singlet in the ($\parallel,\parallel$) configurations. In both cases the ($1\bar{1}0$) face was used. The frequencies of the phonon under stress were obtained from the Fano fits to the line shape, while those of the local mode showed little difference between the peak frequency and that obtained from the fits, so the peak frequencies were used in Fig. 7(b).

The frequency shifts and splittings for both the local mode and the phonon have the same qualitative features: The split components appear in the same polarizations, with the doublet at a higher frequency than the singlet for [001] stress and the reverse for [111] stress. The striking difference between them is that the hydrostatic shift of the local mode per unit stress is about 2.6 times that of the optic phonon. The hydrostatic shift is related to the mode Grüneisen parameter, defined as[15]

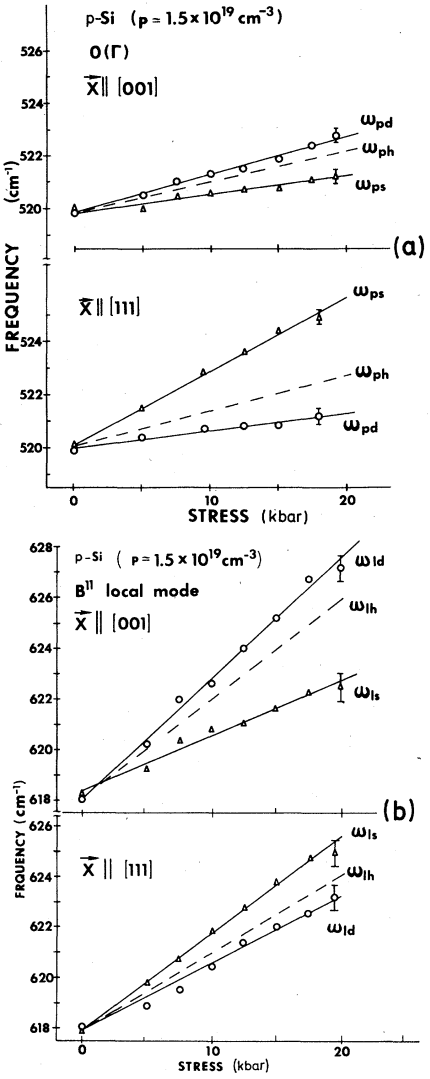

FIG. 7. Frequencies of the optic phonon (a) and local mode (b) as a function of uniaxial stress.

$$\gamma_i = \frac{3}{\chi_t \omega_i} \frac{\partial \omega_i}{\partial X} . \tag{19}$$

Using $\chi_t = 1.012 \times 10^{-12}$ cm^2/dyn as the isothermal compressibility[15] of Si, ω_i the frequency of the mode, and the hydrostatic shift per unit stress $\partial\omega_i/\partial X$, we obtain $\gamma_L = 1.64 \pm 0.25$ for the local mode of ^{11}B and $\gamma_p = 0.75 \pm 0.06$ for the optic phonon, both for a concentration of $p = 1.5 \times 10^{19}$ cm^{-3}. The large value of γ_L as compared to γ_p is, we believe, due to the large local compressibility in the vicinity of the smaller boron atom, which has an ionic radius[18] of 0.82 Å as compared to 1.11 Å for Si.

The expected change in the local compressibility can be estimated as follows: using Murnaghan's[19] equation,

$$P = \frac{B_0}{B_0'}\left[\left(\frac{a_0}{a}\right)^{3B_0'} - 1\right], \tag{20}$$

where P is the pressure, B_0 is the bulk modulus at zero pressure, B_0' is the derivative of B_0 with respect to P (equal to ~4 for this family of materials[20]) and a and a_0 are the perturbed and unperturbed lattice parameters, respectively, we find

$$B = -a\frac{dP}{3da} = +B_0\left(\frac{a_0}{a}\right)^{3B_0'} . \tag{21}$$

We assume that if boron were to crystallize in a tetrahedral structure it would have the bulk modulus of its neighbor in the Periodic Table (diamond) scaled by the appropriate ionic radius according to Eq. (21). Using the bulk modulus of diamond (4.42×10^{12} dyn/cm^2) and the atomic radii[18] $R_c = 0.77$ and $R_B = 0.82$ we obtain B_0 (boron) $= 2.21 \times 10^{12}$ dyn/cm^2. Furthermore, the compressibility of a Si–B bond can be expected to be proportional to the average of the bulk moduli of boron and silicon, i.e., 1.6×10^{12} dyn/cm^2. This value, however, would correspond to a B–Si spacing of $1.11 + 0.82$ Å instead of the real 2.22 Å. Scaling B by the factor obtained from Eq. (21) yields $B_{(\mathrm{Si-B})} = 0.29 \times 10^{12}$ dyn/cm^2. The ratio of bulk modulus of a Si–B bond to that of a Si–Si bond is 0.29 which is to be compared with the ratio of Grüneisen constants 0.45. The agreement is improved if one uses instead of the Grüneisen parameters the parameters $p + 2q$ related to the Grüneisen parameters through[17]

$$(p + 2q) = 6\omega_i^2 \gamma . \tag{22}$$

The parameters $p + 2q$ should be directly proportional to the pressure derivatives of the *force constants*. The ratio of $(p + 2q)_p$ to $(p + 2q)_B$ is 0.32 in rather good agreement with the ratio of bulk moduli given above (0.29).

The Fano interaction under high uniaxial stresses is stronger for the doublet component of the optic phonon than for singlet and this tends to lower the frequency of the doublet at high stresses, resulting in a lowering of the hydrostatic shift which we have computed by the center of gravity rule. This is borne out by the lower γ_p (0.74) in the heavily doped Si as compared with[10] $\gamma_p \simeq 0.9$ in pure Si. A similar effect is expected in the case of the local mode. However, to the best of our knowledge, γ_L has not been measured in a compensated crystal where no free carriers are present. Measurements on a sample of lower doping where the Fano interaction is small are difficult owing to the weaker intensities.

The local mode of the ^{10}B isotope was found to remain at a frequency 24 ± 1 cm^{-1} higher than the ^{11}B isotope under uniaxial stress within the limits

TABLE IV. Coefficients describing the shift and splitting of the optic phonon and local mode of ^{11}B under uniaxial stress for a carrier concentration of $p = 1.5\times10^{19}$ cm^{-3}. The coefficients for the optic phonon in pure Si are listed for comparison. All the coefficients are in units of 10^{28} sec^{-2}.

Coefficient	Pure Si optic phonon[a]	Doped Si $p = 1.5\times10^{19}$ cm^{-3} Optic phonon	Doped Si $p = 1.5\times10^{19}$ cm^{-3} ^{11}B local mode
$p+2q$	-5.20 ± 0.26[b]	-3.99 ± 0.2[b]	-14.7 ± 1.5[b]
	-5.33 ± 0.26[c]	-4.47 ± 0.22[c]	-11.8 ± 1.2[c]
p	-1.43 ± 0.07[b]	-1.23 ± 0.06[b]	-3.7 ± 0.4[a]
q	-1.89 ± 0.09[b]	-1.50 ± 0.08[b]	-4.8 ± 0.5[b]
r	-0.53 ± 0.03[c]	-0.64 ± 0.03[c]	-0.39 ± 0.04[c]

[a] Reference 17.
[b] Measured under [001] stress.
[c] Measured under [111] stress.

of experimental error. The coefficients describing the splitting of the zone-center optic phonon and the local mode of ^{11}B under uniaxial stress,[17] defined in Appendix B of Ref. 12 are listed in Table IV. For comparison the same coefficients measured in pure Si for the optic phonon are also listed.

ACKNOWLEDGMENTS

One of the authors (H.R.C.) would like to thank the Alfred P. Sloan Foundation for financial support.

*Work partly performed at Max-Planck-Institut für Festkörperforschung, 7000 Stuttgart 80, Federal Republic of Germany.
[1] P. G. Dawber and R. J. Elliott, Proc. R. Soc. London Ser. A 273, 222 (1963); Proc. Phys. Soc. London, 81, 453 (1963).
[2] M. Balkanski and W. J. Nazarewicz, J. Phys. Chem. Solids 25, 437 (1964); 27, 671 (1966).
[3] J. F. Angress, A. R. Goodwin, and S. D. Smith, Proc. R. Soc. London Ser. A 287, 64 (1965).
[4] R. Beserman, M. Jouanne, and M. Balkanski, *Proceedings of the Eleventh International Conference on the Physics of Semiconductors* (P. W. N.—Polish Scientific Publishers, Warsaw, 1972), p. 1181.
[5] F. Cerdeira, T. A. Fjeldly, and M. Cardona, Phys. Rev. B 9, 4344 (1974).
[6] U. Fano, Phys. Rev. 124, 1866 (1961). Discrete-continuum interaction of the Fano-type has also been observed in other Raman work. See, for instance, D. L. Rousseau and S. P. S. Porto, Phys. Rev. Lett. 20, 1354 (1968); A. Zawadowski and J. Ruvalds, *ibid.* 24, 1111 (1970); J. F. Scott, T. C. Damen, J. Ruvalds, and A. Zawadowski, Phys. Rev. B 3, 1295 (1971); R. S. Katiyar, J. F. Ryan, and J. F. Scott, *ibid.* B 4, 2635 (1971).
[7] F. Cerdeira, T. A. Fjeldly, and M. Cardona, Phys. Rev. B 8, 4734 (1973), and references therein.
[8] H. Vogelmann and T. A. Fjeldly, Rev. Sci. Instrum. 45, 309 (1974).
[9] Syton, a trademark of the Monsanto Corporation.
[10] M. V. Klein, in *Light Scattering in Solids*, edited by M. Cardona (Springer, New York, 1975), p. 147.
[11] P. Lawaetz, doctoral thesis, Technical University of Denmark, 1978 (unpublished).
[12] M. Chandrasekhar, J. B. Renucci, and M. Cardona, Phys. Rev. B 17, 1623 (1978).
[13] L. R. Swanson and A. A. Maradudin, Solid State Commun. 8, 859 (1970).
[14] R. N. Dexter, H. J. Zeiger, B. Lax, Phys. Rev. 104, 637 (1956).
[15] C. Kittel, *Introduction to Solid State Physics* (Wiley, New York, 1971), p. 143.
[16] L. Genzel and M. Cardona (unpublished).
[17] E. Anastassakis, A. Pinczuk, E. Burstein, F. H. Pollak, and M. Cardona, Solid State Commun. 8, 133 (1970).
[18] *Table of Periodic Properties of the Elements* (Sargent Welch, Skokie, Ill., 1968).
[19] F. D. Murnaghan, Proc. Nat. Acad. Sci., U.S.A. 30, 244 (1944).
[20] H. J. McSkimin, A. Jayaraman, and P. Andreatch, J. Appl. Phys. 38, 2362 (1967).